NeuroImage xxx (2015) xxx–xxx

Contents lists available at ScienceDirect

NeuroImage

journal homepage: www.elsevier.com/locate/ynimg

T2 quantification from only proton density and T2-weighted MRI by modelling actual refocusing angles

Kelly C. McPhee [a,*], Alan H. Wilman [a,b]

[a] Department of Physics, University of Alberta, 4-181 CCIS, Edmonton, Alberta T6G 2E1, Canada
[b] Department of Biomedical Engineering, University of Alberta, 1098 RTF, Edmonton, Alberta T6G 2V2, Canada

ARTICLE INFO

Article history:
Received 28 January 2015
Accepted 26 May 2015
Available online xxxx

Keywords:
Fast spin echo
T2-weighting
Proton density
R2 quantification
Stimulated echoes
ISEC

ABSTRACT

Proton density and transverse relaxation (T2)-weighted fast spin echo images are frequently acquired. T2 quantification is commonly performed by applying an exponential fit to these two images, despite recent evidence that an exponential fit is insufficient to correctly quantify T2 in the presence of imperfect RF refocusing due to standard 2D slice selection or use of reduced refocusing angles. Here we examine the feasibility of accurate two echo fitting using standard proton density and T2-weighted images by utilizing Bloch equation simulations and prior knowledge of refocusing angles. This method is demonstrated in simulation, phantom, and human brain experiments, in comparison to the exponential approach, and to a 32 echo multiple-echo spin echo approach. Comparison to single spin echo is also performed in phantom experiments. The two echo method, which compensates for indirect and stimulated echoes, enables accurate quantitative T2 over a wide range of flip angle and T2 values using standard MRI methods, provided there is adequate SNR and flip angle knowledge.

Introduction

Quantification of transverse relaxation time (T2) has been used to probe tissues in the brain (MacKay et al., 2006, 2009; Schenck and Zimmerman, 2004; Vymazal et al., 1996; Lebel et al., 2012; Deoni, 2010) and body (Alústiza et al., 2004; Dunn et al., 2004; Giri et al., 2009; Matzat et al., 2013; Verhaert et al., 2011; Maas et al., 2014) yielding information related to tissue properties such as water, macromolecular, or iron content. The quantitative nature of T2 improves comparisons between subjects or within subjects over time by removing signal variations found in T2-weighted images, such as those dependent on receiver gain or flip angle variation. Multiple-echo spin echo (MESE) techniques are the standard method of measuring T2, however, acquisition of full MESE data sets is not always feasible due to time constraints.

Proton density (PD) and T2-weighted fast spin echo (FSE) (often referred to as TURBO spin echo, or RARE) (Hennig et al., 1986) are frequently performed in clinical research studies, and T2-weighted FSE is typically included in most clinical brain exams. The resulting weighted images provide useful image contrast, however additional value could be obtained by quantifying T2. Many studies have used PD and T2-weighted images to estimate T2 using a simple exponential fit (Gibbs et al., 2001; Liney et al., 1996; Bauer et al., 2010, 2014; Hasan et al., 2009, 2010; Tanabe et al., 1998; He and Parikh, 2013). However, imperfect refocusing due to slice profiles, RF interference or purposeful reduction in refocusing angles all result in stimulated or indirect echoes, which contaminate the exponential T2 decay (Majumdar et al., 1986a, 1986b; Hennig, 1991; Lebel and Wilman, 2010), and compromise exponential T2 fitting.

Using exponential fitting, differences between T2 values obtained from MESE experiments and pairs (or sets) of FSE images have been previously noted (Leppert et al., 2009; Roebuck et al., 2009). In addition, inter-site studies have noted systematic differences between sites and vendors in T2 maps calculated from exponential fitting of pairs of PD and T2-weighted images (Bauer et al., 2010). Exponential fitting does not take into account key differences in RF pulse sequence parameters (pulse shape, relative refocusing width, refocusing angle, spoiling) between various scanners/vendors, which affect the degree of stimulated and indirect echo contamination. Furthermore, a two point fitting approach is expected to be more sensitive to pulse sequence specific errors than a multi-echo approach, since less data is being used which precludes averaging of errors across multiple time points. These errors include varying stimulated and indirect echo contributions, as well as signal-to-noise (SNR) effects, which all complicate the accurate fitting of T2 using only two echoes.

The goal of this work is to demonstrate that a PD and a T2-weighted image may be used to accurately determine the T2 through advanced fitting of the typically non-exponential decay. Direct fitting of the spin response for T2 quantification is an area of active research using methods such as stimulated echo compensation with echo phase graph (Lebel and Wilman, 2010; Prasloski et al., 2012; Rooney et al., 2011; Huang et al., 2013, 2014; Uddin et al., 2013), or full Bloch

* Corresponding author.
E-mail addresses: kcmcphee@gmail.com (K.C. McPhee), wilman@ualberta.ca (A.H. Wilman).

http://dx.doi.org/10.1016/j.neuroimage.2015.05.079
1053-8119/

modelling (Ben-Eliezer et al., 2014). These methods rely on multiple echoes to obtain satisfactory fitting conditions for three fitting parameters (T2, flip angle, initial signal amplitude), which requires multiple echoes (in practice, at least four (Uddin et al., 2013), but typically many more). Here, we examine the case of only two echoes (PD and T2-weighted) using simulation, phantom and human brain experiments. Unlike the original implementation of stimulated echo compensation (Lebel and Wilman, 2010) which used Fourier transform approximation of slice profile and multiple echoes, the two point method introduced here requires precise modelling of RF pulse response and prior knowledge of the refocusing flip angles.

Methods

A Bloch equation model was used to determine T2 from only a PD-weighted and a T2-weighted FSE image and prior flip angle knowledge, which was achieved with a flip angle map. Modelling of the spin response accounts for all echo pathways, providing indirect and stimulated echo compensation (ISEC). Using both simulations and human brain experiments, this two echo ISEC method was tested using a range of echo times against exponential fitting, and compared to a standard MESE approach using 32 echoes with ISEC T2 fitting. Additionally, two point fitting was investigated using the second echo, instead of the first PD-weighted echo, and a later echo.

T2 fitting model

Simulations of slice-selective T2 signal amplitudes (both MESE and FSE) were performed using the Shinnar-Le Roux (SLR) algorithm (Pauly et al., 1991) to simulate RF pulses, and solutions to the Bloch equations to simulate relaxation, similar to Ben-Eliezer et al. (2014). All simulations and image processing were performed using custom in-house MATLAB (R2014a, 64 bit) programs. In order to model slice selection, magnetization vectors were calculated at 1001 points equally spaced over twice the excitation width in the slice-select direction. RF pulses were modelled using 1024 points equally spaced over the duration of the pulse. RF pulse profiles, flip angles, gradients and timing were simulated according to their respective pulse sequence parameters.

Slice selective MESE and FSE data were fitted for T2 and amplitude via minimization of the sum squared difference between experimental and simulated data. Flip angle maps were separately measured and provided to the fitting algorithm. A dictionary of decay curves with many T2 and flip angle values was created prior to fitting (similar to Parker et al., 2001; Ben-Eliezer et al., 2014). Voxel-wise fitting was performed using a subset of curves from the dictionary with excitation and refocusing flip angles which correspond to the measured value at that voxel. The dictionary of curves was specific to the parameters used to acquire the data (RF pulse shapes and timing, gradient amplitudes, crusher gradients, and echo spacing).

To create a dictionary of curves for T2 fitting, simulations were repeated for a range of T2 (10–1000 ms at 0.1 ms resolution up to 150 ms, 1 ms resolution from 150–200 ms, 2 ms resolution from 200–300 ms, 5 ms resolution from 300–500 ms, and 10 ms resolution from 500–1000 ms), and normalized flip angle values (0.20–1.80 at 0.005 resolution, resulting in refocusing angles from 36–324°), and an assumed T1 of 2 s. The dictionary contained a total of over 510,000 curves, allowing for precise fitting. The range of T1 values at 4.7 T is expected to typically be 1.0–2.0 s (Takaya et al., 2004; Thomas et al., 2005; Jezzard et al., 1996) in most brain tissue. The impact of T1 choice is examined.

Flip angle mapping with slice profile correction

Flip angle maps were computed using a double angle method (Stollberger and Wach, 1996), accounting for slice profile effects. Correction for slice profile is necessary to avoid errors in the flip angle map (Bouhrara and Bonny, 2012). Two FSE images were acquired with nominal excitation angles of 60° and 120°, both with the same refocusing train, effective TE 43 ms, TR 7 s, echo train length 24, and echo spacing 10.75 ms. RF pulse shapes, slice thickness, field of view, and matrix size were matched to the corresponding T2 mapping sequence. SLR simulations of the FSE imaging sequence for nominal excitation angles of 60° and 120°, and for many RF amplitude values, were performed. The relationship between RF amplitude, and the ratio of signal magnitudes from the two images, S(120°)/S(60°) was fitted with a ninth degree polynomial, which was used to rapidly generate a corrected flip angle map from acquired data. Resulting flip angle maps are median filtered with a 5 × 5 pixel filter before input into the T2 fitting algorithm.

Flip angle map values are expressed as a normalized parameter. We define the normalized flip angle map values, nB1, according to: $\alpha = \mathrm{nB1} \cdot \alpha_{\mathrm{nom}}$, where α is the flip angle achieved at the centre of the selected slice, α_{nom} is the prescribed nominal flip angle, and nB1 is the scaling factor relating the two angles.

In vivo experiments

Axial single-slice two dimensional MESE and FSE images of the human brain were acquired in six healthy volunteers (aged 29 ± 6 years) through iron-rich deep grey matter on a 4.7 T (Varian Inova) MRI system. All subjects provided written, informed consent and this investigation was approved by the local institutional ethics board. MESE sequences were acquired with TR 4 s, TE 10–320 ms, constant echo spacing 10 ms, echo train length 32, excitation and refocusing pulse durations 4 ms and 1.6 ms, excitation width 4 or 5 mm, refocusing width 1.75× excitation width, Gaussian pulse shapes (time-bandwidth product 2.69; 5 sigma width), matrix 256 × 145 × 1; voxel size = 1 × 1.25 × 4 mm^3. Eight FSE images were acquired with effective TE (10, 20, 30, 40, 50, 60, 70, or 80 ms), prescribed excitation 90°, refocusing 180°, with RF pulses and timing, TR, and resolution matched to the multi-echo experiment. FSE images for flip angle mapping were acquired with resolution, and pulse shapes matched to MESE data.

T2 maps were computed using the ISEC model described in Section 2.1, using the independently measured flip angle map, and various sequence and echo combinations to determine optimal parameters. Fitting was performed with the full 32 echo MESE data set, all eight FSE images, and various pairs of FSE images. FSE pairs made use of the first or second echo (effective TE = 10 or 20 ms), paired with later T2-weighted echoes (effective TE = 40 ms to 80 ms, with constant 10 ms echo spacing). For comparison, data were also fitted with an exponential model.

Regions-of-interest (ROIs) were drawn selecting six bilateral grey matter regions (putamen, globus pallidus, head of the caudate nucleus, thalamus, cortical grey matter, and insular cortex) and two bilateral white matter regions (frontal and posterior white matter). Mean ROI T2 values were reported, with bilateral ROIs combined.

Phantom validation

In order to validate the ISEC method, phantom measurements were performed with comparison to a single spin echo, which exhibits no stimulated echoes due to its use of only 1 refocusing pulse. Six solutions with $MnCl_2$ concentrations ranging from 28 to 512 mM were placed in 28 mm diameter (55 ml) cylindrical plastic laboratory tubes. T1 and T2 were measured with inversion recovery, and single spin echo experiments. Ten single spin echo experiments were performed (TE = 13.1, 20, 30, 40, 50, 60, 70, 80, 130, 200 ms; TR 14 s; nominal excitation 90°; nominal refocusing 180°; sinc pulse shapes). T2 maps were computed from this single spin echo data using an exponential fit. T1 values were estimated with an inversion recovery experiment (inversion times = 14, 20, 50, 100, 200, 300, 500, 1000, 2000, 3000, 4000 ms; FSE readout; 8 mm slice thickness; TR 12 s; TE 8.5 ms; matrix 192 × 256; FOV 26 × 20 cm).

Please cite this article as: McPhee, K.C., Wilman, A.H., T2 quantification from only proton density and T2-weighted MRI by modelling actual refocusing angles, NeuroImage (2015), http://dx.doi.org/10.1016/j.neuroimage.2015.05.079

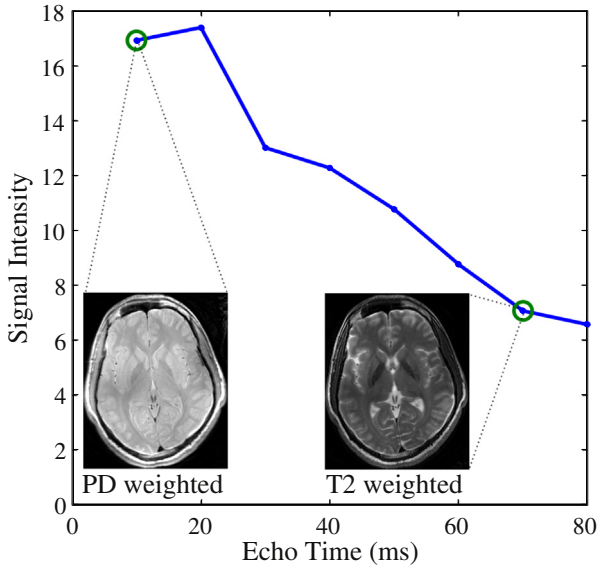

Fig. 1. T2 decay is non-exponential. An example decay curve (data point chosen from the caudate head; T2 = 60.5 ms, measured refocusing angle = 168°), is shown with the corresponding PD and T2-weighted images.

MESE, eight FSE images, and a nB1 map were also acquired in the same scanning session, with parameters matched to in vivo experiments, with the following exceptions: 8 mm slice thickness for all experiments, and TR = 14 s for nB1 mapping. T2 maps using both exponential and ISEC fits were computed from MESE data, and from different combinations of pairs of FSE images. Results were compared to single spin echo T2 fits.

Numerical validation: Uncertainty due to noise

In order to determine the optimal pair of effective echoes in simulation, SNR analysis was performed. The coefficient of variation in resulting T2 fit values for 500 samples with simulated SNR of 50 for a range of T2 values (20–100 ms), nB1 values (0.5–1.5, i.e. refocusing angles from 90° to 270°), and various choices of echo combinations was computed. Analysis was repeated for a range of SNR values (3–300), for T2 = 50 ms and nB1 = 1.0 (corresponding to a refocusing angle of 180°), with 1000 samples at each SNR. Here, SNR is defined as simulated signal magnitude in the first echo relative to standard deviation of the noise. Random Gaussian complex noise was added to complex simulated decay curves, with fitting performed on the resulting simulated noisy magnitude data. Maps of the uncertainty in resulting T2 fits (coefficient of variation, in percent) were computed for various combinations of echoes. For all simulations, pulse shapes, gradients, and timing were matched to human experimental parameters.

Numerical validation: Assumption of uniform T1

To validate, and to assess error in the two point ISEC fitting with respect to the constant T1 assumption, simulated T2 decay curves with T1 = 1.0 s were fitted with a dictionary which used a T1 of 2 or 3 s. A range of simulated data was used with various combinations of echo times (constant echo spacing of 10 ms), T2 values (10–150 ms) and nB1 (0.5–1.5, corresponding to refocusing angles of 90–270°). Errors from exponential fit results were also examined.

To further explore the repercussions of an assumption of a uniform T1 value, decay curves were simulated with a range of T1 values (300–3000 ms) and were fitted using the two point ISEC method, assuming T1 = 2 s, as was assumed for in vivo experiments. Errors were examined for a range of T2 (25–300 ms) and nB1 (0.33–1.5, corresponding to 60–270° refocusing angles) values. Fitting was performed using the two point ISEC method with echoes 1 and 7 (effective TE 10, 70 ms), echoes 2 and 6 (effective TE 20, 60 ms), and again for the 32 echo MESE method (TE = 10, 20, …, 320 ms).

Results

The goal of this work is clarified in Fig. 1, whereby a PD and a T2-weighted image are used to determine T2 through advanced fitting of the typically non-exponential decay. The echo contamination is clearly evident in the non-exponential multiple-echo decay, beginning with an enhanced second echo. However, the acquisition of only a PD and a T2-weighted image, do not provide visible evidence of the contaminating echo signals. Thus two echoes may be fit with an exponential with minimal fitting errors, but producing an incorrect result.

In vivo T2 mapping

T2 values computed using the two point ISEC averaged over six healthy volunteers are reported in Table 1 for various possible echo combinations. T2 values derived from FSE values are reported as relative percent to ISEC fit of MESE data. The refocusing angle, α_R, within each

Table 1
Group averaged T2 values using ISEC fitting.[a,b]

	Thalamus	Globus pallidus	Caudate head	Putamen	Insular cortex	Cortical GM	Posterior WM	Frontal WM
MESE (ms)	52.3 ± 3.3	34.3 ± 2.2	57.9 ± 2.1	51.1 ± 3.4	72.6 ± 3.0	55.4 ± 4.4	59.7 ± 6.5	52.4 ± 3.1
nB1	1.13 ± 0.02	1.09 ± 0.06	1.04 ± 0.06	1.03 ± 0.05	0.99 ± 0.04	0.87 ± 0.06	0.92 ± 0.05	0.86 ± 0.07
α_R	203.6° ± 4.4°	196.6° ± 10.3°	186.6° ± 10.0°	186.0° ± 9.0°	178.3° ± 6.4°	157.4° ± 10.1°	166.2° ± 9.3°	154.9° ± 13.5°
FSE data set	*Percentage T2 fit accuracy (relative to gold standard MESE, %)*							
Echo 1–8 (TE 10–80 ms)	94 ± 3	99 ± 6	98 ± 6	98 ± 8	97 ± 5	96 ± 5	96 ± 5	96 ± 5
Echo 1, 3 (TE 10, 30 ms)	90 ± 2	96 ± 8	96 ± 8	95 ± 9	89 ± 1	91 ± 11	87 ± 2	105 ± 19
Echo 1, 4 (TE 10, 40 ms)	90 ± 2	95 ± 9	95 ± 9	95 ± 10	89 ± 3	92 ± 8	89 ± 6	95 ± 9
Echo 1, 5 (TE 10, 50 ms)	97 ± 5	101 ± 8	99 ± 8	100 ± 10	95 ± 3	95 ± 8	95 ± 4	102 ± 11
Echo 1, 6 (TE 10, 60 ms)	92 ± 2	97 ± 7	94 ± 5	96 ± 9	91 ± 6	94 ± 8	92 ± 5	95 ± 7
Echo 1, 7 (TE 10, 70 ms)	97 ± 4	104 ± 7	100 ± 8	100 ± 10	98 ± 6	98 ± 6	98 ± 5	100 ± 7
Echo 1, 8 (TE 10, 80 ms)	94 ± 4	97 ± 6	98 ± 7	97 ± 8	100 ± 5	95 ± 8	95 ± 5	96 ± 7
Echo 2, 4 (TE 20, 40 ms)	88 ± 3	94 ± 8	93 ± 5	92 ± 8	90 ± 4	94 ± 3	91 ± 9	83 ± 5
Echo 2, 5 (TE 20, 50 ms)	99 ± 8	102 ± 7	99 ± 6	98 ± 8	98 ± 3	97 ± 5	98 ± 6	95 ± 5
Echo 2, 6 (TE 20, 60 ms)	91 ± 3	97 ± 8	93 ± 4	95 ± 8	92 ± 6	95 ± 4	94 ± 7	89 ± 4
Echo 2, 7 (TE 20, 70 ms)	98 ± 5	104 ± 7	100 ± 6	99 ± 9	100 ± 6	100 ± 5	100 ± 6	96 ± 4
Echo 2, 8 (TE 20, 80 ms)	94 ± 5	97 ± 7	97 ± 6	96 ± 7	102 ± 6	96 ± 6	97 ± 6	92 ± 4

[a] Gold standard T2 fit values from ISEC fitting of MESE data are reported as mean (ms) ± standard deviation within the group. All other T2 values are expressed as the relative value compared to the gold standard (%).
[b] n = 6 subjects, aged 29.0 ± 6.2 years.

Please cite this article as: McPhee, K.C., Wilman, A.H., T2 quantification from only proton density and T2-weighted MRI by modelling actual refocusing angles, NeuroImage (2015), http://dx.doi.org/10.1016/j.neuroimage.2015.05.079

Table 2
Group averaged T2 values using exponential fit.[a,b]

	Thalamus	Globus pallidus	Caudate head	Putamen	Insular cortex	Cortical GM	Posterior WM	Frontal WM
MESE, ISEC fit (ms)	52.3 ± 3.3	34.3 ± 2.2	57.9 ± 2.1	51.1 ± 3.4	72.6 ± 3.0	55.4 ± 4.4	59.7 ± 6.5	52.4 ± 3.1
MESE, exponential fit (ms)	41.9 ± 34.3	31.0 ± 22.0	49.0 ± 34.7	42.3 ± 30.1	59.4 ± 42.2	48.1 ± 34.4	51.0 ± 36.6	44.4 ± 31.4
nB1	1.13 ± 0.02	1.09 ± 0.06	1.04 ± 0.06	1.03 ± 0.05	0.99 ± 0.04	0.87 ± 0.06	0.92 ± 0.05	0.86 ± 0.07
α_R	203.6° ± 4.4°	196.6° ± 10.3°	186.6° ± 10.0°	186.0° ± 9.0°	178.3° ± 6.4°	157.4° ± 10.1°	166.2° ± 9.3°	154.9° ± 13.5°
FSE data set	*Percentage T2 fit accuracy (relative to gold standard MESE, %)*							
Echo 1–8 (TE 10–80 ms)	128 ± 3	134 ± 6	128 ± 6	128 ± 7	128 ± 5	128 ± 4	125 ± 6	129 ± 4
Echo 1, 3 (TE 10, 30 ms)	189 ± 9	159 ± 13	200 ± 13	177 ± 12	212 ± 7	185 ± 12	167 ± 10	356 ± 66
Echo 1, 4 (TE 10, 40 ms)	175 ± 5	160 ± 10	179 ± 12	169 ± 11	184 ± 9	177 ± 10	165 ± 18	189 ± 13
Echo 1, 5 (TE 10, 50 ms)	148 ± 6	140 ± 8	148 ± 10	143 ± 10	151 ± 4	143 ± 9	142 ± 11	158 ± 10
Echo 1, 6 (TE 10, 60 ms)	143 ± 4	142 ± 9	142 ± 8	141 ± 9	143 ± 8	143 ± 7	138 ± 10	148 ± 8
Echo 1, 7 (TE 10, 70 ms)	136 ± 4	136 ± 8	137 ± 9	133 ± 10	139 ± 7	135 ± 5	133 ± 9	140 ± 6
Echo 1, 8 (TE 10, 80 ms)	135 ± 4	137 ± 8	137 ± 8	134 ± 8	145 ± 7	135 ± 6	133 ± 8	139 ± 6
Echo 2, 4 (TE 20, 40 ms)	94 ± 2	105 ± 7	97 ± 4	97 ± 7	91 ± 4	97 ± 3	94 ± 8	88 ± 4
Echo 2, 5 (TE 20, 50 ms)	97 ± 7	104 ± 7	97 ± 6	97 ± 8	93 ± 3	95 ± 4	96 ± 6	93 ± 5
Echo 2, 6 (TE 20, 60 ms)	103 ± 3	113 ± 8	102 ± 5	105 ± 7	98 ± 6	104 ± 3	102 ± 6	99 ± 4
Echo 2, 7 (TE 20, 70 ms)	104 ± 4	112 ± 7	105 ± 6	105 ± 8	102 ± 5	104 ± 5	104 ± 5	101 ± 3
Echo 2, 8 (TE 20, 80 ms)	108 ± 4	117 ± 7	109 ± 5	109 ± 7	111 ± 5	108 ± 4	108 ± 5	105 ± 3

[a] Gold standard T2 fit values from ISEC fitting of MESE data are reported as mean (ms) ± standard deviation within the group. T2 values resulting from two point fits are expressed as the relative value compared to the gold standard (%).
[b] n = 6 subjects, aged 29.0 ± 6.2 years.

region is also reported, as derived from the flip angle maps. The use of first and seventh echo (TE = 10 and 70 ms) produce the best two-echo results with ISEC fitting. Corresponding T2 values from the same regions, but derived from exponential fitting are reported in Table 2. In exponential fitting, use of the first echo (PD-weighted) image gives very poor results, but better results are achieved using the second echo combined with a later echo.

Example T2 maps from sequences using nominal 180° refocusing pulses and the corresponding normalized B1 map are shown in Fig. 2. The T2 map computed using ISEC and the 32 echo MESE data set (a) or FSE images (b, c) makes use of the independently measured flip angle map (d). T2 maps computed using an exponential fit are shown below (e, f). The T2 maps shown used fits from the optimal FSE pair for ISEC (TE 10 and 70 ms) and for exponential (TE 20 and 60 ms), as determined from Tables 1 and 2.

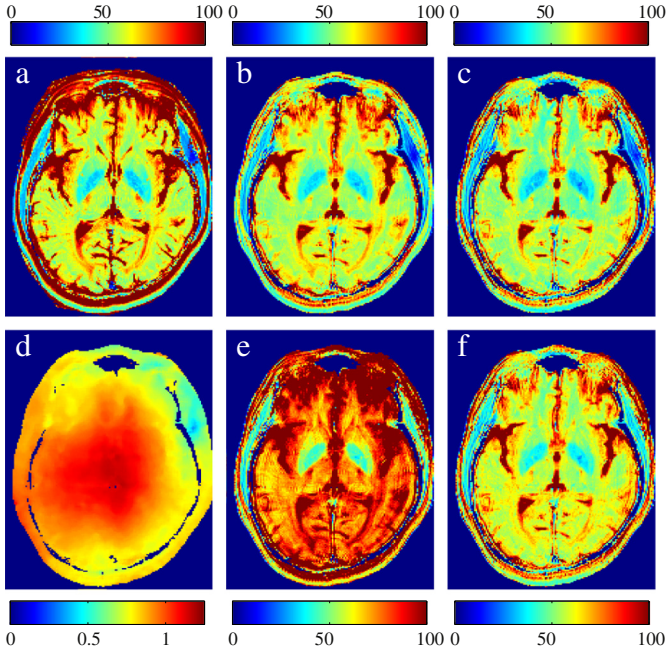

Fig. 2. Comparing T2 maps from ISEC and exponential fit. T2 maps (ms) computed using ISEC: (a) 32 echo MESE experiment, (b) two FSE images TE = 10 and 70 ms, (c) TE = 20 and 60 ms. Exponential T2 fitting with two FSE images (e) TE = 10 and 70 ms, (f) TE = 20 and 60 ms. (d) Independently measured nB1 map used for fits a–c. All FSE and MESE data shown were acquired with a nominal 180° refocusing pulse and 10 ms echo spacing.

Phantom validation

T2 fit results from single spin echo measurements, and from ISEC and exponential fitting of MESE and pairs of FSE images are reported in Table 3. T1 values from inversion recovery are also reported. Phantom results show excellent agreement between ISEC methods and single spin echo results across a wide range of T2 values. Exponential fits of FSE and MESE data overestimate T2 results in most cases.

Numerical assessment of T2 fitting

Uncertainty in the T2 measurement is examined in Fig. 3 by mapping the coefficient of variance in T2 fitting results from 500 simulated data sets using an SNR of 50. Results are shown for various combinations of echo pairs, for a range of T2 (20–100 ms) and nB1 values (0.5–1.5, resulting in a refocusing angle of 90–270°). SNR simulations show that for experiments where T2 is expected in that range, the optimal TE pair is 10 ms and 70 ms (1st and 7th echoes), which agrees with the in vivo findings from Table 1.

Uncertainty in a T2 measurement for a range of SNR values is examined in Fig. 4, for a simulated T2 of 50 ms, and refocusing angle of 180°. Using ISEC, T2 fit values are increased by approximately 0–3% when SNR >30 (Fig. 4), relative to zero noise simulations. Low SNR value results in a bias to overestimate T2 due to the noise floor. Even at high SNR values, exponential fitting fails to provide accurate results. Even where nB1 = 1 (refocusing angle = 180°), slice profile effects result in indirect and stimulated echo contamination, leading to significant errors in T2 estimation with exponential fitting.

Fig. 5 shows the percent error in T2 fit results across a range of flip angle and T2 values using different pairs of echoes: the first and seventh (a and c), and the second and sixth (b and d). Effects of T1 overestimation are also explored using a 1 or 2 s overestimation of the actual 1 s value. Errors in ISEC T2 fit results are larger when T1 over-estimate increases (Fig. 5, curves where $T_{1,\text{dictionary}} = 3$s). Error curves from exponential fitting where the first and seventh echo are used exceed 30%, and are not shown. When T1 is overestimated by 2 s, errors occur which have a strong flip angle dependence.

Error due to the assumption of a constant T1 is further examined in Fig. 6 using a wide range of simulated T1 from 300 to 3000 ms, while

Please cite this article as: McPhee, K.C., Wilman, A.H., T2 quantification from only proton density and T2-weighted MRI by modelling actual refocusing angles, NeuroImage (2015), http://dx.doi.org/10.1016/j.neuroimage.2015.05.079

Table 3
Phantom T2 values from ISEC and exponential fit.[a]

Sample	1	2	3	4	5	6
[$MnCl_2$] (mM)	27.7	67.9	124.6	270.0	401.5	512.3
T1 (ms)	2055 ± 53	1383 ± 24	912 ± 43	515 ± 16	306 ± 21	353 ± 7
nB1	1.11 ± 0.03	1.17 ± 0.03	1.20 ± 0.05	1.01 ± 0.04	0.90 ± 0.03	1.03 ± 0.04
α_R	200° ± 5°	211° ± 6°	217° ± 10°	183° ± 8°	161° ± 6°	186° ± 8°
T2 values from various fitting methods and data sets (ms)						
Single spin echo	239 ± 11	108 ± 3	53.2 ± 2.2	26.4 ± 1.4	17.6 ± 0.2	13.7 ± 0.5
MESE (ISEC)	227 ± 5	98 ± 2	50.6 ± 2.4	24.6 ± 0.9	17.3 ± 0.5	13.2 ± 0.7
MESE (exponential)	267 ± 7	124 ± 4	68.8 ± 3.7	32.9 ± 1.3	24.6 ± 0.9	19.3 ± 1.0
FSE echo 1, 7 I.E. fit	220 ± 40	101 ± 8	51.3 ± 3.4	25.8 ± 2.1	16.2 ± 2.5	13.0 ± 2.0
FSE echo 2, 6 I.E. fit	192 ± 19	94 ± 6	52.5 ± 3.5	25.1 ± 1.9	15.6 ± 2.2	11.8 ± 2.0
FSE echo 1, 7 exponential fit	893 ± 704	187 ± 24	79.0 ± 7.2	31.7 ± 2.6	19.2 ± 3.1	14.8 ± 3.2
FSE echo 2, 6 exponential fit	180 ± 14	99 ± 6	59.5 ± 3.6	29.8 ± 1.9	20.8 ± 1.9	17.3 ± 2.1

[a] Values are reported as mean ± standard deviation within the ROI.

assuming a constant T1 of 2 s. Error is shown as a function of T2 and refocusing flip angle for two point ISEC fit using the first and seventh echo. Error maps from using ISEC fitting on the second and sixth echo, and with 32 echoes contained the same features, with similar resulting fit error (within 0.5% for the majority of T1 and refocusing values), and are not shown. In general, error in the T2 measurement was found to be less than 2% when the T1 estimate was within 1 s of the actual value when refocusing angles exceeded 85°. Over-estimate of T1 by ≤1.5 s caused less than 2% error in T2 measurement error when the refocusing angle was near 180°. The importance of an accurate T1 estimate increases with increased stimulated echoes.

Discussion

The two point ISEC method described here enables accurate T2 quantification from only two FSE images (PD and T2-weighted) by modelling the pulse sequence, taking into account stimulated and indirect echoes via prior knowledge of the flip angles and slice profiles. Human brain T2 values obtained from the two point FSE method with ISEC fitting (Table 1) agreed very well (within 4% for most combinations of data) with the T2 results from ISEC fitting of the 32 echo MESE data set. In phantom experiments, T2 values from both ISEC fitting of two echoes and MESE data sets agreed within uncertainty with T2 measurements from single spin echo experiments.

Exponential fits of the MESE and FSE data were not as robust (Table 2). The two point exponential fits of PD (TE = 10 ms) weighted and T2-weighted images grossly overestimated T2 values (33–112%, depending on chosen echo times), as expected from simulations.

However, exponential fits of in vivo experiments with certain combinations of data showed reasonable T2 values (Table 2). In particular, when the second echo (TE = 20 ms) is combined with a later echo, the exponential T2 map is much closer to the gold standard values. However, the echo time of the second echo is too late for a true PD-weighted image. Furthermore, the T2 map is visibly warmer on the color scale (Fig. 2f), and resulting values within ROIs are typically found to be larger, compared to ISEC fitting of the MESE data (Table 2). The error in exponential fitting results depended on both T2 and refocusing angle, when the second echo is paired with a later echo. Regions with shorter T2 values (less than ~50 ms) typically overestimated T2, while moderate T2 values (50–80 ms) seemed to be near gold standard values. Conventionally, one may assume that using only even pairs of echoes would be sufficient to minimize stimulated echo effects; however, we have found that this approach does not remove errors, as T1 contamination is introduced via alternate echo pathways.

Knowledge of the actual flip angle and RF pulse shapes are an essential part of this advanced fitting method. The flip angle knowledge removes a parameter from the fitting process, which enables only two points to yield an accurate solution. Accurate knowledge of the flip angle and slice profile allow for appropriate compensation of indirect and stimulated echo pathways. At high magnetic field, an actual flip angle map was needed due to substantial in-plane RF variation. However at lower fields, with RF variation reduced, a flip angle map may not be necessary. At any field strength, knowledge of the RF pulse shape is required for the simulation process. If the RF pulse shapes are not provided by the vendor, they may be measured using a digital oscilloscope.

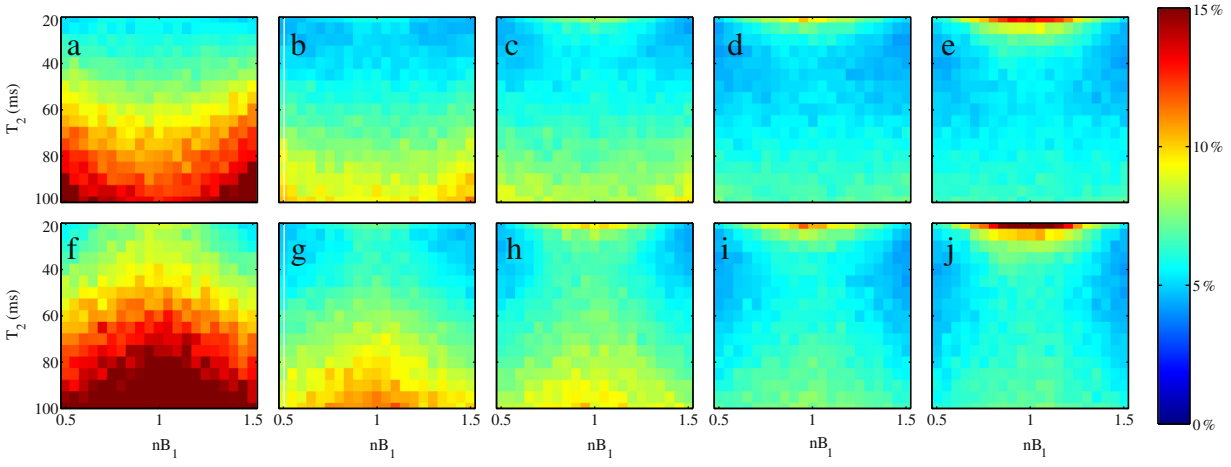

Fig. 3. Examining instability in two point ISEC fitting. Coefficient of variance (%) in ISEC T2 fitting results for simulated SNR of 50 are shown for a range of T2 and nB1 values, and the following echo pairs: (a) 10 and 40 ms, (b) 10 and 50 ms, (c) 10 and 60 ms, (d) 10 and 70 ms, (e) 10 and 80 ms, (f) 20 and 40 ms, (g) 20 and 50 ms, (h) 20 and 60 ms, (i) 20 and 70 ms, (j) 20 and 80 ms.

Please cite this article as: McPhee, K.C., Wilman, A.H., T2 quantification from only proton density and T2-weighted MRI by modelling actual refocusing angles, NeuroImage (2015), http://dx.doi.org/10.1016/j.neuroimage.2015.05.079

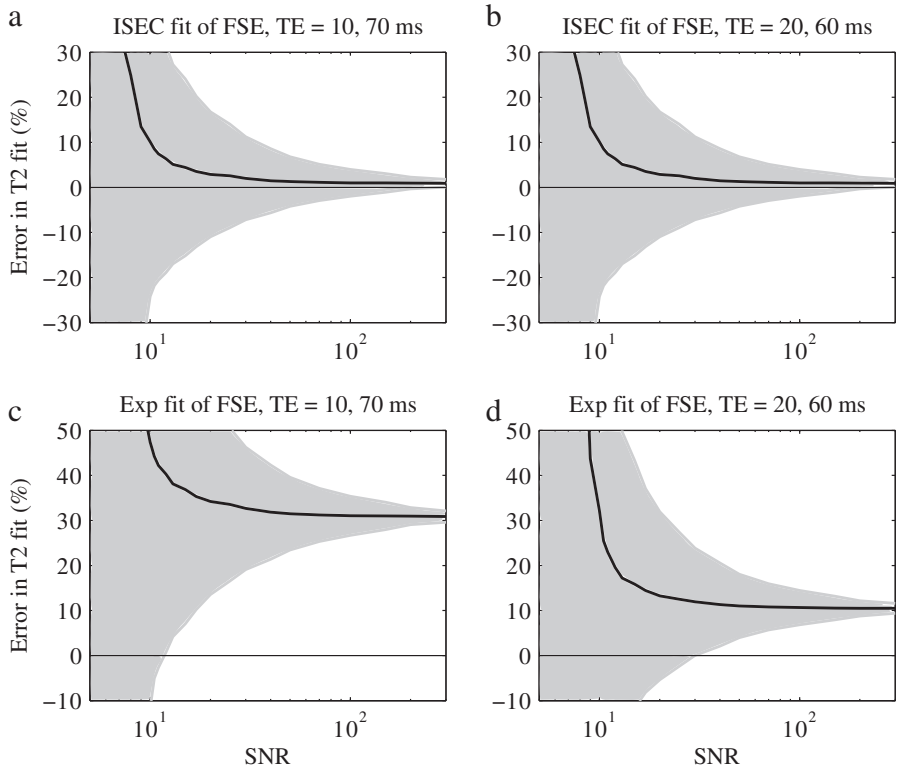

Fig. 4. Examining SNR limitations. Mean ± standard deviation in T2 fitting error for simulated T2 of 50 ms and nB1 of 1.0 (refocusing angle of 180°) are shown for two echo choices using either (a,b) ISEC or (c,d) exponential (Exp) fitting. Mean lines are shown in black, with plus/minus one standard deviation limits shaded in grey. In general, T2 is overestimated by 0–3% with ISEC fitting when SNR >30.

SNR simulations show that for T2 between 20 and 100 ms, the optimal pair of effective TEs for ISEC fitting is 10 ms and 70 ms, which is supported by in vivo results (Table 1). Using a combination of images with TEs of 10 ms and 50 or 60 ms also performs well if T2 is between 20 and 50 ms, however, the accuracy of larger T2 values is compromised. Other combinations of FSE images could provide accurate measurements, though the accuracy depends on the TEs, and the T2 range expected. The pair of images chosen here compromises between accuracy of specific T2 values, and accuracy over the desired range of T2 values. For other applications, a different T2 weighting may be optimal. However, for clinical applications, the choice of TE of PD and T2 weighting are usually fixed, with PD being the first echo and T2-weighted using TE of 60–100 ms (Bauer et al., 2010; Hasan et al., 2009, 2010; Tanabe et al., 1998). The values found to be optimal here fall within that range.

Without previous T1 measurement, an assumption of T1 is required in calculation of the fitting model. We found that errors due to the T1 assumption were small when the T1 of the model was within 1 s of the actual T1 value (Figs. 5 and 6). Errors increase with increased stimulated echo contributions, and, when the T1 assumption is inaccurate (particularly when overestimated by 2 s), resulting errors vary significantly with refocusing angle (Fig. 5) due to varied contributions from indirect and stimulated echo pathways. The original implementation of ISEC found T2 measurement to be relatively insensitive to T1 when the T1/T2 ratio is large (Lebel and Wilman, 2010), however that work used a 20 echo MESE data set, allowing for averaging of T1 error across 20 points and only 10 ms between measured points. In the two point approach, the points may be 60 ms apart (10 and 70 ms). Furthermore, the amount of T1 contamination varies with refocusing flip angle and the number of RF pulses that spins have experienced, and therefore does not contribute equally to all possible effective echo times, resulting in potential increases in error in two point fitting. We find that, when the difference between actual and assumed T1 values in fitting is greater than 1 s, errors with strong dependence on refocusing angle can occur (see Fig. 5, curves where the assumed T1 = 3 s). Estimating T1 to within 1 s is generally straightforward for healthy tissues. However, inclusion of an approximate T1 map could aid pathological T2 measurements.

The only difference between the pairs of FSE acquisitions used for two point ISEC fitting in this work was the effective TE, with all other parameters kept consistent. In practice, TR, echo spacing, echo train length, or other parameters might differ between PD and T2-weighted images, which would compromise the approach used here, although potential corrections might be possible. For example, if TR is changed between sequences, this could lead to different initial magnetization in each acquisition, and result in substantial errors in T2 estimation, unless a correction factor was included for different TRs which would require knowledge of T1. Alternatively, one could use a dual echo protocol to maintain the same TR for both images, and minimize total acquisition time.

This work builds on previous implementations of spin response fitting for T2 mapping by Lebel and Wilman (2010), and Ben-Eliezer et al. (2014). These methods fit simultaneously for T2, flip angle, and a scaling parameter from MESE data. In order to fit for T2 from only two data points, the flip angle must be measured separately. The Lebel method underestimates nB1 (Lebel and Wilman, 2010) due to the slice profile approximation, and restricts fitting of nB1 to less than 1. Symmetry around nB1 of 1 is assumed, but has since been shown not to be the case (Breitkreutz et al., 2013). When providing a flip angle map to a T2 fit which accounts for stimulated echoes, accurate simulations of decay curves including flip angles and slice profiles are required. In this work, we make use of the Shinnar-Le Roux algorithm for simulation of slice selective RF pulses and Bloch simulations for decay curves in order to fully simulate signal intensities of FSE images and avoid making approximations for slice profile effects.

In clinical practice, lower refocusing angles are typically used due to specific absorption rate constraints. With lower refocusing angles,

Please cite this article as: McPhee, K.C., Wilman, A.H., T2 quantification from only proton density and T2-weighted MRI by modelling actual refocusing angles, NeuroImage (2015), http://dx.doi.org/10.1016/j.neuroimage.2015.05.079

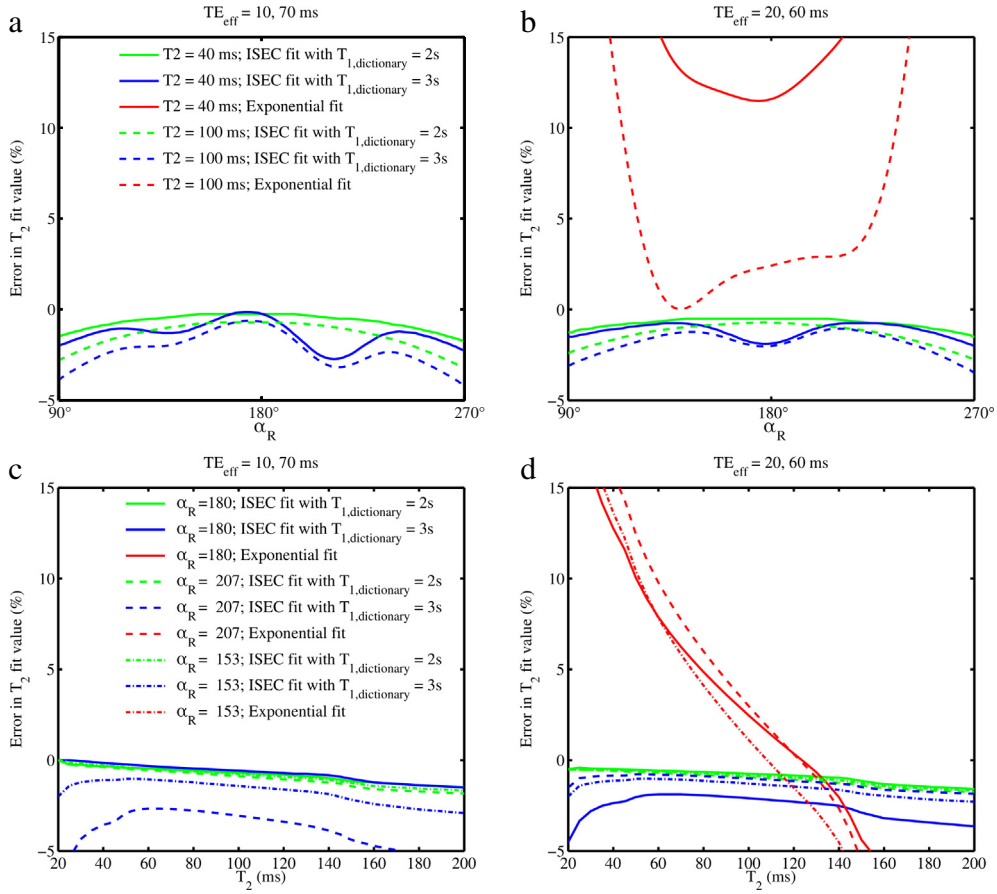

Fig. 5. Examining T2 fit accuracy. T2 fitting accuracy is examined for a range of T2 and refocusing angles (α_R) using only two echo times: (a, c) 10 and 70 ms (1st and 7th echo), and (b, d) 20 and 60 ms (2nd and 6th echo). Here, T1 is simulated to be 1.0 s, but the lookup table used for fitting assumes 2 or 3 s. In (a, c), the exponential fit is off the graph due to errors exceeding 30%.

stimulated echo contamination will increase, resulting in an increase in errors in exponential fitting over those examined here. Further, clinical sequences may have increased amounts of stimulated echo contributions due to the use of narrow refocusing widths relative to the excitation width. Here, we have used a refocusing slice of 1.75× excitation width, which helps to reduce non-exponential echo contamination.

This work was performed using a single slice acquisition. It is readily extendible to multi-slice protocols, provided SNR is sufficient. Previous work has found that incidental magnetization transfer (MT) does not significantly affect grey matter T2 values, however a reduction in SNR was observed (Uddin et al., 2013). For white matter, increased delay between off-resonant RF pulses and on-resonant readout processes minimizes differential MT effects between myelin water and other pools, due to exchange (Vavasour et al., 2000).

The limitations of the method quantified here are specific to the acquisition parameters (in particular, pulse shapes and timing, and echo time). For example, the use of 3D sequences may limit the effects of slice selection profile, and experiments at standard 1.5 T may limit

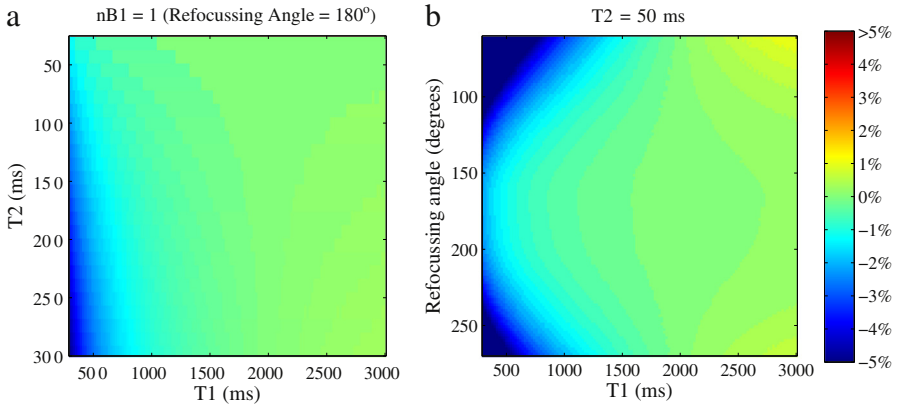

Fig. 6. T2 error maps examining uniform T1 assumption. Error due to the assumption of a global T1 value is examined in the two point ISEC, where echoes 1 and 7 (TE = 10, 70 ms) were used. A range of T2, nB1 and T1 were simulated, and fit, assuming a global T1 of 2 s. Error in the resulting T2 fit is shown for (a) nB1 = 1, and a range of actual T1 and T2 values, and (b) T2 = 50 ms, and a range of actual T1 and nB1 values.

Please cite this article as: McPhee, K.C., Wilman, A.H., T2 quantification from only proton density and T2-weighted MRI by modelling actual refocusing angles, NeuroImage (2015), http://dx.doi.org/10.1016/j.neuroimage.2015.05.079

in-plane flip angle variations. Nevertheless, any use of imperfect or non-180° refocusing angles can cause stimulated and indirect echo pathways. Simulations and experiments indicate that exponential fits using the PD (first echo) image are insufficient for T2 quantification, with errors depending on both the flip angle, and T2 value (Fig. 5). The experiments here used nominal refocusing angles of 180°, which varied up to 30% across the brain in a single experiment, due to high field (4.7 T) interference effects. Simulations indicate that much lower refocusing angles would result in even poorer two echo exponential fitting performance (Fig. 5).

In addition to allowing for rapid T2 quantification in future studies, this method potentially allows for retrospective studies on existing databases that contain PD and T2-weighted images, where flip angle maps are also available or can be predicted. Studies such as that by Bauer et al. (2010) have attempted exponential fitting of PD and T2-weighted images for T2 quantification, but found systematic differences when trying to combine data from multiple sites. This is likely due to different refocusing pulse shapes and angles, to which exponential fitting is highly sensitive. The experiments and simulations here included nominal 180° refocusing pulse trains, though a range of potential refocusing angles were examined. In clinical applications, lower refocusing pulses, or variable refocusing pulse trains may be used, further increasing the likelihood of seriously compromised results from exponential fitting.

Conclusions

In conclusion, ISEC fitting of a PD and a T2-weighted FSE image allows for accurate T2 fitting. By incorporating the actual refocusing angle into the fitting process, ISEC fitting achieves a two point fit while providing much greater accuracy and less sensitivity to refocusing pulse shape and angle than exponential fitting. This method can enable accurate quantitative T2 mapping, without the need of a specialized T2 mapping acquisition, by utilizing existing PD and T2-weighted images with known flip angles.

Acknowledgments

We would like to thank Peter Seres for assistance with data collection.

Grant support was provided by Natural Sciences and Engineering Council of Canada (NSERC) and the Canadian Institutes of Health Research. Salary support for KCM was provided by an NSERC scholarship.

References

Alústiza, J.M., Artetxe, J., Castiella, A., Agirre, C., Emparanza, J.I., Otazua, P., García-Bengoechea, M., Barrio, J., Mújica, F., Recondo, J.A., 2004. MR quantification of hepatic iron concentration1. Radiology 230 (2), 479–484 (Feb.).

Bauer, C.M., Jara, H., Killiany, R., and Alzheimer's Disease Neuroimaging Initiative, 2010. Whole brain quantitative T2 MRI across multiple scanners with dual echo FSE: applications to AD, MCI, and normal aging. NeuroImage 52 (2), 508–514 (Aug.).

Bauer, S., Wagner, M., Seiler, A., Hattingen, E., Deichmann, R., Nöth, U., Singer, O.C., 2014. Quantitative T2'-mapping in acute ischemic. Stroke 45 (11), 3280–3286 (Nov.).

Ben-Eliezer, N., Sodickson, D.K., Block, K.T., 2014. Rapid and accurate T2 mapping from multi-spin-echo data using bloch-simulation-based reconstruction: mapping using bloch-simulation-based reconstruction. Magn. Reson. Med. 73 (2), 809–817 (Mar.).

Bouhrara, M., Bonny, J.M., 2012. B1 mapping with selective pulses. Magn. Reson. Med. 68 (5), 1472–1480 (Nov.).

Breitkreutz, D., McPhee, K.C., Wilman, A.H., 2013. Value of independent flip angle mapping for transverse relaxometry with stimulated echo compensation. Proceedings of the 21st annual meeting of the International Society for Magnetic Resonance in Medicine, p. 2466 (Salt Lake City, Utah, USA).

Deoni, S.C., 2010. Quantitative relaxometry of the brain. Top. Magn. Reson. Imaging 21 (2), 101–113 (Apr.).

Dunn, T.C., Lu, Y., Jin, H., Ries, M.D., Majumdar, S., 2004. T2 relaxation time of cartilage at MR imaging: comparison with severity of knee osteoarthritis. Radiology 232 (2), 592–598 (Aug.).

Gibbs, P., Tozer, D.J., Liney, G.P., Turnbull, L.W., 2001. Comparison of quantitative T2 mapping and diffusion-weighted imaging in the normal and pathologic prostate. Magn. Reson. Med. 46 (6), 1054–1058 (Dec).

Giri, S., Chung, Y.C., Merchant, A., Mihai, G., Rajagopalan, S., Raman, S.V., Simonetti, O.P., 2009. T2 quantification for improved detection of myocardial edema. J. Cardiovasc. Magn. Reson. 11 (1), 56 (Dec.).

Hasan, K.M., Halphen, C., Kamali, A., Nelson, F.M., Wolinsky, J.S., Narayana, P.A., 2009. Caudate nuclei volume, diffusion tensor metrics, and T2 relaxation in healthy adults and relapsing-remitting multiple sclerosis patients: implications to understanding gray matter degeneration. J. Magn. Reson. Imaging 29 (1), 70–77 (Jan.).

Hasan, K.M., Walimuni, I.S., Kramer, L.A., Frye, R.E., 2010. Human brain atlas-based volumetry and relaxometry: application to healthy development and natural aging. Magn. Reson. Med. 64 (5), 1382–1389 (Nov.).

He, L., Parikh, N.A., 2013. Automated detection of white matter signal abnormality using T2 relaxometry: application to brain segmentation on term MRI in very preterm infants. NeuroImage 64, 328–340 (Jan.).

Hennig, J., 1991. Echoes—how to generate, recognize, use or avoid them in MR-imaging sequences. Part II: echoes in imaging sequences. Concepts Magn. Reson. 3 (4), 179–192 (Oct.).

Hennig, J., Nauerth, A., Friedburg, H., 1986. RARE imaging: a fast imaging method for clinical MR. Magn. Reson. Med. 3 (6), 823–833 (Dec.).

Huang, C., Bilgin, A., Barr, T., Altbach, M.I., 2013. T2 relaxometry with indirect echo compensation from highly undersampled data. Magn. Reson. Med. 70 (4), 1026–1037 (Oct.).

Huang, C., Altbach, M.I., El Fakhri, G., 2014. Pattern recognition for rapid T2 mapping with stimulated echo compensation. Magn. Reson. Imaging 32 (7), 969–974 (Sep.).

Jezzard, P., Duewell, S., Balaban, R.S., 1996. MR relaxation times in human brain: measurement at 4 T. Radiology 199 (3), 773–779 (Jun.).

Lebel, R.M., Wilman, A.H., 2010. Transverse relaxometry with stimulated echo compensation. Magn. Reson. Med. 64 (4), 1005–1014 (Oct.).

Lebel, R.M., Eissa, A., Seres, P., Blevins, G., Wilman, A.H., 2012. Quantitative high-field imaging of sub-cortical gray matter in multiple sclerosis. Mult. Scler. 18 (4), 433–441 (Apr.).

Leppert, I.R., Almli, C.R., McKinstry, R.C., Mulkern, R.V., Pierpaoli, C., Rivkin, M.J., Pike, G., 2009. T2 relaxometry of normal pediatric brain development. J. Magn. Reson. Imaging 29 (2), 258–267 (Feb.).

Liney, G.P., Knowles, A.J., Manton, D.J., Turnbull, L.W., Blackband, S.J., Horsman, A., 1996. Comparison of conventional single echo and multi-echo sequences with a fast spin-echo sequence for quantitative T2 mapping: application to the prostate. J. Magn. Reson. Imaging 6 (4), 603–607 (Jul.-Aug.).

Maas, M.C., Vos, E.K., Lagemaat, M.W., Bitz, A.K., Orzada, S., Kobus, T., Kraff, O., Maderwald, S., Ladd, M.E., Scheenen, T.W.J., 2014. Feasibility of T2-weighted turbo spin echo imaging of the human prostate at 7 tesla. Magn. Reson. Med. 71 (5), 1711–1719 (May).

MacKay, A., Laule, C., Vavasour, I., Bjarnason, T., Kolind, S., Mädler, B., 2006. Insights into brain microstructure from the T2 distribution. Magn. Reson. Imaging 24 (4), 515–525 (May).

MacKay, A.L., Vavasour, I.M., Rauscher, A., Kolind, S.H., Mädler, B., Moore, G.R., Traboulsee, A.L., Li, D.K., Laule, C., 2009. MR relaxation in multiple sclerosis. Neuroimaging Clin. N. Am. 19 (1), 1–26 (Feb.).

Majumdar, S., Orphanoudakis, S.C., Gmitro, A., O'Donnell, M., Gore, J.C., 1986a. Errors in the measurements of T2 using multiple-echo MRI techniques. I. Effects of radiofrequency pulse imperfections. Magn. Reson. Med. 3 (3), 397–417 (Jun.).

Majumdar, S., Orphanoudakis, S.C., Gmitro, A., O'Donnell, M., Gore, J.C., 1986b. Errors in the measurements of T2 using multiple-echo MRI techniques. II. Effects of static field inhomogeneity. Magn. Reson. Med. 3 (4), 562–574 (Aug.).

Matzat, S.J., van Tiel, J., Gold, G.E., Oei, E.H.G., 2013. Quantitative MRI techniques of cartilage composition. Quant. Imaging Med. Surg. 3 (3), 162–174 (Jun.).

Parker, G.J.M., Barker, G.J., Tofts, P.S., 2001. Accurate multislice gradient echo T1 measurement in the presence of non-ideal RF pulse shape and RF field nonuniformity. Magn. Reson. Med. 45 (5), 838–845 (May).

Pauly, J., Le Roux, P., Nishimura, D., Macovski, A., 1991. Parameter relations for the shinnar-le roux selective excitation pulse design algorithm [NMR imaging]. IEEE Trans. Med. Imaging 10 (1), 53–65 (Mar.).

Prasloski, T., Mädler, B., Xiang, Q.S., MacKay, A., Jones, C., 2012. Applications of stimulated echo correction to multicomponent T2 analysis. Magn. Reson. Med. 67 (6), 1803–1814 (Jun.).

Roebuck, J.R., Haker, S.J., Mitsouras, D., Rybicki, F.J., Tempany, C.M., Mulkern, R.V., 2009. Carr-purcell-meiboom-gill imaging of prostate cancer: quantitative T2 values for cancer discrimination. Magn. Reson. Imaging 27 (4), 497–502 (May).

Rooney, W.D., Poolaro, J.R., Forbes, S.C., Wang, D.J., Vanderborne, K., Walter, G.A., 2011. Application of the extended phase graph technique to improve T2 quantitation across sites. Proceedings of the 19th annual meeting of the International Society for Magnetic Resonance in Medicine Annual Meeting, p. 138 (Montreal, Canada).

Schenck, J.F., Zimmerman, E.A., 2004. High-field magnetic resonance imaging of brain iron: birth of a biomarker? NMR Biomed. 17 (7), 433–445 (Nov.).

Stollberger, R., Wach, P., 1996. Imaging of the active B1 field in vivo. Magn. Reson. Med. 35 (2), 246–251 (Feb.).

Takaya, N., Watanabe, H., Mitsumori, F., 2004. Elongated T1 values in human brain and the optimization of MDEFT measurements at 4.7T. Proceedings of the 12th Annual Meeting of the International Society for Magnetic Resonance in Medicine, p. 2339 (Kyoto, Japan).

Tanabe, J.L., Vermathen, M., Miller, R., Gelinas, D., Weiner, M.W., Rooney, W.D., 1998. Reduced MTR in the corticospinal tract and normal T2 in amyotrophic lateral sclerosis. Magn. Reson. Imaging 16 (10), 1163–1169 (Dec.).

Thomas, D.L., De Vita, E., Deichmann, R., Turner, R., Ordidge, R.J., 2005. 3D MDEFT imaging of the human brain at 4.7 T with reduced sensitivity to radiofrequency inhomogeneity. Magn. Reson. Med. 53 (6), 1452–1458 (Jun.).

Please cite this article as: McPhee, K.C., Wilman, A.H., T2 quantification from only proton density and T2-weighted MRI by modelling actual refocusing angles, NeuroImage (2015), http://dx.doi.org/10.1016/j.neuroimage.2015.05.079

Uddin, M.N., Lebel, R.M., Wilman, A.H., 2013. Transverse relaxometry with reduced echo train lengths via stimulated echo compensation. Magn. Reson. Med. 70 (5), 1340–1346 (Nov.).

Vavasour, I.M., Whittall, K.P., Li, D.K., MacKay, A.L., 2000. Different magnetization transfer effects exhibited by the short and long t2 components in human brain. Magn. Reson. Med. 44 (6), 860–866 (Dec.).

Verhaert, D., Thavendiranathan, P., Giri, S., Mihai, G., Rajagopalan, S., Simonetti, O.P., Raman, S.V., 2011. Direct T2 quantification of myocardial edema in acute ischemic injury. J. Am. Coll. Cardiol. Img. 4 (3), 269–278 (Mar.).

Vymazal, J., Brooks, R.A., Baumgarner, C., Tran, V., Katz, D., Bulte, J.W.M., Bauminger, E.R., Chiro, G.D., 1996. The relation between brain iron and NMR relaxation times: an in vitro study. Magn. Reson. Med. 35 (1), 56–61 (Jan.).

Please cite this article as: McPhee, K.C., Wilman, A.H., T2 quantification from only proton density and T2-weighted MRI by modelling actual refocusing angles, NeuroImage (2015), http://dx.doi.org/10.1016/j.neuroimage.2015.05.079